

# Formation of Nitroaromatic Compounds in Advanced Oxidation Processes: Photolysis versus Photocatalysis

JANET DZENGEL, JOERN THEURICH, AND DETLEF W. BAHNEMANN\*

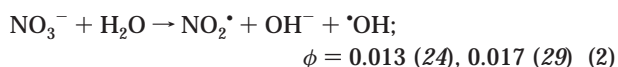
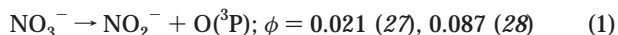
*Institut für Solarenergieforschung GmbH Hameln/Emmerthal, Aussenstelle Hannover, Sokelantstrasse 5, 30165 Hannover, Germany*

There is a growing demand for efficient treatment of organic polluted wastewaters by advanced oxidation processes (AOPs). Besides optimization of the processes, the detailed understanding of degradation mechanisms and interactions of organic pollutants with inorganic substrates is important for technical applications of AOPs. Therefore, the aim of the present study was to investigate the influence of nitrate ions on the photooxidation of phenol for various AOPs at different pH values. Three different oxidation processes were compared in these studies: direct photolysis,  $\text{TiO}_2/\text{UV}$ , and  $\text{H}_2\text{O}_2/\text{UV}$ . Special emphasis has been laid on the analysis of byproducts, especially on the formation of nitroaromatic compounds. The formation of intermediates as well as the depletion of phenol were monitored by HPLC technique. The total organic carbon content, TOC, was measured to monitor the mineralization. Highest degradation rates and lowest concentrations of intermediates were observed with  $\text{TiO}_2/\text{UV}$  being the AOP. Formation of highly toxic nitrophenols was only observed when homogeneous AOPs were employed. For the  $\text{TiO}_2/\text{UV}$  process no formation of nitroaromatic byproducts occurred. At pH 5 formation of nitrophenols was observed employing direct photolysis in the presence of  $\text{NO}_3^-$ , while with  $\text{H}_2\text{O}_2/\text{UV}$  nitrophenols were detected only when the concentration of  $\text{NO}_3^-$  was higher than that of  $\text{H}_2\text{O}_2$ . At pH 11 no nitroaromatic intermediates were found for any AOPs compared in this study.

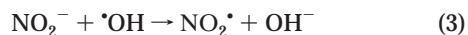
## Introduction

The widespread pollution of ground, surface, and drinking water or effluents from industries and households with hazardous and relatively biostable organic compounds demands an increasing effort toward the development of technologies for the cleanup of such wastewaters (1–5). Alternative processes for the treatment of wastewater and drinking water are the so-called advanced oxidation processes (AOPs), such as ozonation,  $\text{H}_2\text{O}_2/\text{UV}$ , or  $\text{TiO}_2/\text{UV}$  (6–8), which are generally expected to result in the complete destruction of all hazardous compounds. They have attracted a growing scientific and technological interest over the last 20 years, and their applicability for the oxidation of several model pollutants has been experimentally verified (6, 9). Detailed

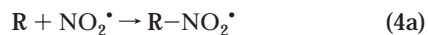
studies focusing on the treatment of real wastewaters (10–16), which often represent very complex systems, have been published less frequently. Especially the reactions between solute molecules, e.g., inorganic salts or humic acids, and organic pollutants have been investigated (to the best of our knowledge) only by a few research groups (7, 17–19). While most of these latter studies were directed toward the inhibiting effect of solutes on the degradation rate of model pollutants (7, 17, 18), possible reactions between the solutes and the contaminants have, in most cases, not attained any attention. However, many solute compounds are themselves able to undergo light-induced chemical reactions, e.g., iron or nitrate (20–22). Especially the latter one is known as a natural source for the photolytic generation of hydroxyl radicals in aquatic environments (23, 24). Its photochemistry has been extensively studied and was recently reviewed by Wagner et al. and by von Sonntag and co-workers (22, 25). Irradiation of nitrate close to its long-wavelength absorption band ( $\epsilon_{302} = 7.1 \text{ M}^{-1} \text{ cm}^{-1}$  (26)) results in two primary photochemical processes: the formation of nitrite ions and atomic oxygen (eq 1) and the formation of  $\text{NO}_2^{\cdot-}$  and  $\cdot\text{OH}$  radicals (eq 2).



Thus, nitrate could in principle promote the efficiency of an AOP by the additional formation of  $\cdot\text{OH}$  radicals, but on the other hand, nitrate ions can also act as an inner filter reducing the available amount of photons suitable to initiate the desired photochemical oxidation of organic contaminants. Furthermore, some of the photoproducts of the nitrate photolysis are able to compete with the pollutants for hydroxyl radicals: e.g., nitrite ions will react in a diffusion-controlled charge-transfer reaction with  $\cdot\text{OH}$  radicals ( $k = 10^{10} \text{ M}^{-1} \text{ s}^{-1}$  (30)) forming hydroxide ions and nitrogen dioxide (eq 3).



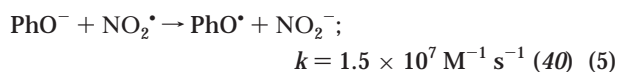
Therefore, it was one aim of the present study to investigate the influence of nitrate ions on the degradation kinetics of the model pollutant phenol comparing different photochemical processes, i.e., direct photolysis,  $\text{H}_2\text{O}_2/\text{UV}$ , and  $\text{TiO}_2/\text{UV}$ . Since nitrogen dioxide is formed as a radical intermediate during the photolysis of nitrate ions (cf. eq 2), the formation of nitroorganic byproducts initiated by the scavenging of the  $\text{NO}_2^{\cdot-}$  radical by organic compounds (eq 4a) or by a reaction of the  $\cdot\text{OH}$  adduct of a substrate molecule with nitrogen dioxide (eq 4b) can be envisaged. These reactions will be competing with the “classical” reactions of  $\text{NO}_2^{\cdot-}$  radicals in the aqueous phase.



However, the formation of nitroorganic compounds via aqueous-phase reactions of  $\text{NO}_2^{\cdot-}$  radicals with organic substrates has so far been reported in the literature—to the best of our knowledge—only for the direct photolysis of hydroxybiphenyls and biphenyls (31–34) or benzene and phenol (35, 36), respectively. During the gas-phase degradation of aromatic hydrocarbons by hydroxyl radicals in the presence of  $\text{NO}_x$ , the formation of nitroaromatic compounds

\* To whom correspondence should be addressed: phone: (+49 +511)35850137; fax: (+49 +511)35850110; e-mail: ISFH.Bahnnemann@oln.comlink.apc.org.

has, on the other hand, been observed, and a reaction scheme involving reaction 4b has been proposed (37–39). Therefore, it was another purpose of the present study to investigate whether also in the aqueous phase reactions 4a and 4b may be able to compete with the well-known electron-transfer reaction from an organic substrate, e.g., phenol, to nitrogen dioxide (eq 5).



## Experimental Methods

**Reagents.** All chemicals were of reagent grade and used without further purification. The water employed in this study was purified by a Milli-Q/RO system (Millipore). P25 from Degussa was used as the  $\text{TiO}_2$  photocatalyst. It consists of 75% anatase and 25% rutile with a specific BET surface area of  $50 \text{ m}^2 \text{ g}^{-1}$  and a primary particle size of 20 nm (41, 42).

**Procedures.** Stock solutions of phenol containing the desired concentration of 1 mM were prepared in water. The photochemical reactor was made of duran glass with a plain quartz window (through which the parallel light beam entered) equipped with a magnetic stirring bar, a water-circulating jacket, and five openings for electrodes and gas supplies. For the irradiation experiments 150 mL of the desired solution was filled into the reactor. The required amount of photocatalyst ( $5 \text{ g L}^{-1}$ ) or  $\text{H}_2\text{O}_2$  (10 mM) and different concentrations of  $\text{KNO}_3$  (0, 10, or 100 mM) were added prior to irradiation. The solution was stirred for at least 30 min in the dark to allow equilibration of the system. To ensure a constant pH value throughout the experiment a pH-stat technique was employed. Details about this technique have been reported elsewhere (43). To guarantee a constant  $\text{O}_2$  concentration, the suspensions were continuously purged with molecular oxygen throughout each experiment. Control experiments performed in the dark showed no observable loss of phenol or intermediates due to stripping effects. However, volatilization of unidentified intermediates upon irradiation cannot be excluded. Irradiations were carried out using a high-pressure mercury lamp (Osram HBO 500W). IR radiation and short-wavelength UV radiation were eliminated by a 10-cm water filter. For the photocatalytic degradation experiments with  $\text{TiO}_2$ , a 320-nm cutoff filter was used to avoid any direct excitation of phenol and nitrate. Samples (5 mL) were taken before and in regular intervals during the irradiation. If required, they were centrifuged with a Heraeus Sepatech Labufuge GL before analyses. Actinometry was performed using Aberchrome 540 (44) in order to determine the total incident light intensity in the wavelength region between 310 and 370 nm which can be absorbed by  $\text{TiO}_2$ . Light of higher and lower wavelength was filtered by means of a UG 5 filter (Schott). The light intensity throughout all experiments in this study was between 330 and  $300 \mu\text{mol}$  of photons  $\text{L}^{-1} \text{ min}^{-1}$ . The photonic efficiency  $\zeta$  was calculated as the ratio of the photocatalytic degradation rate of phenol or TOC and the incident light intensity (45). Its validity for a better comparison of photocatalytic systems has been experimentally verified in several papers recently published (46, 47). For each experiment the degradation rate of the total organic carbon (TOC) was determined from the initial slope of the TOC concentration (measured in terms of mM “ $\text{C}_6$ ”) versus time profiles or for the model pollutant itself from the slope of a plot of the natural logarithm of the phenol concentration as a function of the irradiation time.

**Analyses.** The concentrations of phenol and its reaction intermediates were measured by HPLC (Dionex 4500i) equipped with a reversed-phase column ET 250/8/4 Nucleosil 10  $\text{C}_{18}$ , 10- $\mu\text{m}$  particle size (Macherey & Nagel), or a

TABLE 1. HPLC Retention Times of Intermediates and Model Compounds

compound	retention time (min)	
	Macherey & Nagel	Merck
nitrate	2.39	2.25
1,2,3-trihydroxybenzene	2.81	2.75
1,2,4-trihydroxybenzene	2.89	2.84
hydroquinone	3.05	3.12
hydroxybenzoquinone	3.56	3.35
benzoquinone	4.05	4.34
catechol	4.10	4.82
phenol	6.30	7.40
4-nitrophenol	9.65	11.37
4,4'-dihydroxybiphenyl	12.13	14.53
2-nitrophenol	13.30	18.90

LiChrospher RP-18, 5- $\mu\text{m}$  particle size (Merck), respectively. All substances were detected employing a UV detector at 270 nm. The eluent consisted of a binary mixture of water (containing 1 vol % acetic acid) and methanol (60:40 by volume), and the flow rate was  $1 \text{ mL min}^{-1}$ . Peaks were identified by comparison with retention times of external standards. Table 1 summarizes the measured retention times for various compounds. Concentrations of phenol and intermediates were calculated by calibration curves obtained from HPLC measurements of the respective compound at different concentrations. Peaks which were assigned to commercially unavailable compounds (trihydroxybiphenyl) were not considered for quantitative analysis, except for hydroxybenzoquinone which was treated according to the benzoquinone calibration multiplied by the ratio of the molar absorptivities of hydroxybenzoquinone and benzoquinone at 270 nm ( $\text{BQ}, \epsilon_{270} = 3100.0 \text{ L mol}^{-1} \text{ cm}^{-1}$ ;  $\text{HBQ}, \epsilon_{270} = 7600.0 \text{ L mol}^{-1} \text{ cm}^{-1}$ ). The latter value was derived from a recently published paper by von Sonntag et al. (48). Total organic carbon was measured with a Shimadzu TOC 500 analyzer directly injecting the aqueous solutions after centrifugation.

## Results

**pH Effect.** Even though it is a frequently studied reaction in photocatalysis, no uniform information concerning the optimum pH for the photocatalytic degradation of phenol with titanium dioxide could be extracted from the literature. While several research groups observed highest degradation rates at pH 3.3 (49–51), other groups reported a maximum value at pH 5.5 (52) and 8.0 (53), respectively. Therefore, the influence of the pH on the photonic efficiency of the phenol degradation kinetics as well as for the overall mineralization was determined in a range between pH 3 and 11 (Figure 1). It is obvious that the efficiency for both phenol and TOC removal decreases with increasing pH. While  $\zeta$  decreases by a factor of 3 for the depletion of the model pollutant itself when the pH is raised from pH 3 to 11, it even decreases by a factor of 7 for the overall mineralization. Throughout the entire pH range investigated, the mineralization rate is always smaller than the oxidation rate of phenol and the mineralization is more strongly influenced by a pH change than the oxidation of phenol itself. Thus, higher concentrations of intermediates and/or a slower phenol degradation are expected consequences of the decreasing mineralization rate for neutral and alkaline pH values. This behavior is illustrated in Figure 2 where the sum of the concentrations of all detected intermediates is plotted as a function of the converted phenol. The total amount of detected intermediates increases as the pH is changed from pH 3 to 7 before it decreases again for pH 9 and 11. The numbers inserted in Figure 1 are the calculated values for the ratio of the photonic efficiency of the phenol degradation and its respective overall mineral-

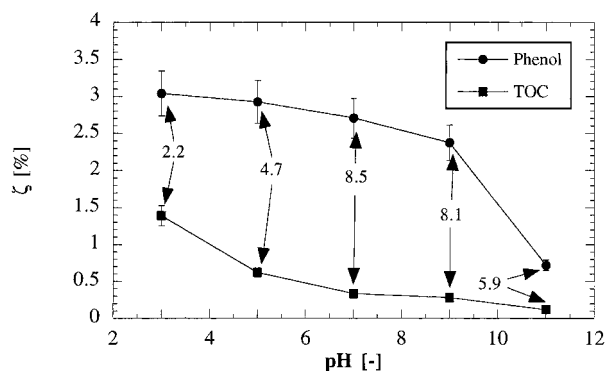


FIGURE 1. Influence of the pH on the photonic efficiency of the photocatalytic phenol and TOC degradation (points represent the mean of three experiments; reproducibility:  $\pm 10\%$ ; the inserted numbers indicate the ratio of the photonic efficiencies of phenol depletion and mineralization). Experimental conditions:  $5 \text{ g L}^{-1}$  Degussa P25,  $1 \text{ mM}$  phenol, continuous  $\text{O}_2$  stream,  $I \sim 320 \mu\text{M min}^{-1}$ ,  $293 \text{ K}$ ,  $V = 150 \text{ mL}$ .

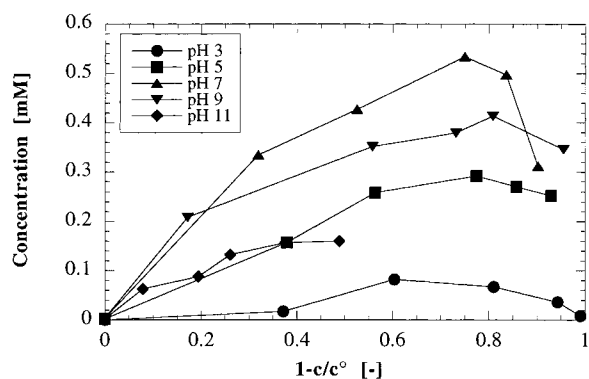


FIGURE 2. Sum of the concentrations of all detected intermediates as a function of the overall amount of converted phenol for different pH values. Experimental conditions:  $5 \text{ g L}^{-1}$  Degussa P25,  $1 \text{ mM}$  phenol, continuous  $\text{O}_2$  stream,  $I \sim 320 \mu\text{M min}^{-1}$ ,  $293 \text{ K}$ ,  $V = 150 \text{ mL}$ , irradiation time =  $300 \text{ min}$ .

ization. It is obvious that this ratio increases up to pH 7 before it decreases for higher pH values. Thus, the decrease in the total amount of detected intermediates for pH 9 and 11 is the expected result, since the rate of mineralization decreases only slowly while that of the depletion of phenol decreases markedly at these higher pH values. However, especially at pH 11 this ratio might be considerably higher, since not all intermediates were identified and the mass balance could not be closed (see also Figure 4). The mechanism of the photocatalytic degradation of phenol has been extensively studied by several research groups (49–53). The most important results of these studies will be briefly summarized at this point to ensure a better understanding of the following experimental approach. The main intermediates identified during the photocatalytic degradation of phenol are hydroquinone (HQ), benzoquinone (BQ), and hydroxybenzoquinone (HBQ). Trihydroxybenzenes (THBenz) are formed as important intermediates especially in the alkaline pH region (49, 53). While catechol (BC) was detected as an intermediate only in small traces in our studies, it was reported by other research groups to be one of the main intermediates in the photocatalytic degradation of phenol (50, 51). It is an important additional result of the present study that the concentrations of all intermediates were found to strongly depend on the reaction pH. A similar behavior has been reported recently for the photocatalytic oxidation of 4-chlorophenol (54, 55) where—besides others—many of the same intermediates were identified.

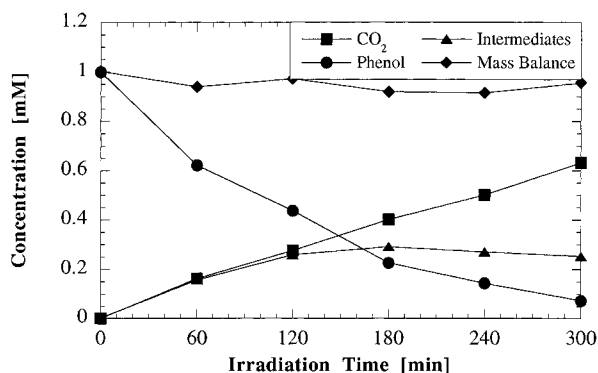


FIGURE 3. Plot of the  $\text{CO}_2$ , phenol, and intermediates-concentration and the mass balance for the photocatalytic degradation of phenol at pH 5. Experimental conditions:  $5 \text{ g L}^{-1}$  Degussa P25,  $1 \text{ mM}$  phenol, continuous  $\text{O}_2$  stream,  $I \sim 320 \mu\text{M min}^{-1}$ ,  $293 \text{ K}$ ,  $V = 150 \text{ mL}$ .

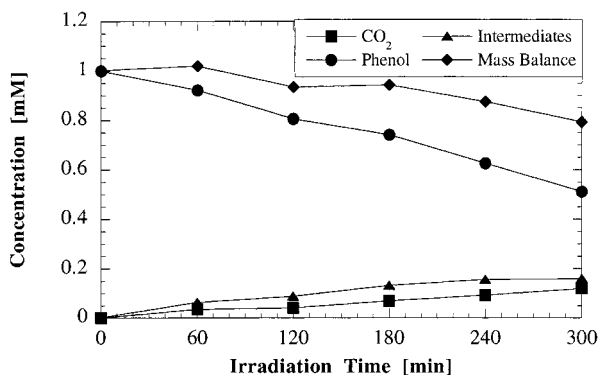


FIGURE 4. Plot of the  $\text{CO}_2$ , phenol, and intermediates-concentration and the mass balance for the photocatalytic degradation of phenol at pH 11. Experimental conditions:  $5 \text{ g L}^{-1}$  Degussa P25,  $1 \text{ mM}$  phenol, continuous  $\text{O}_2$  stream,  $I \sim 320 \mu\text{M min}^{-1}$ ,  $293 \text{ K}$ ,  $V = 150 \text{ mL}$ .

The dependence of the concentration of phenol, the formed carbon dioxide, and the sum of the intermediates is shown together with the mass balance as a function of the irradiation time in Figures 3 and 4 for pH 5 and 11, respectively. While carbon dioxide is formed in a linear fashion over the entire irradiation time for both pH values studied, i.e., obeying zeroth-order kinetics for the overall mineralization, the depletion of phenol itself can best be described by a first-order rate law at pH 5 (the respective semilogarithmic plot is not presented here) exhibiting, however, almost zeroth-order kinetics at pH 11. As was already shown in Figure 1 the destruction of phenol is much faster at pH 5 than at pH 11. Interestingly, the mass balance is constant at about 90% over the entire irradiation time when the reaction is carried out at pH 5, while it decreases slowly at pH 11 starting from almost 100% down to 80% after 5 h of irradiation. Thus, there are considerable concentrations of nondetected (most likely aliphatic ring-opening compounds) or nonquantified intermediates at pH 11, the concentrations and/or stabilities of which are considerably smaller at pH 5.

**Influence of  $\text{NO}_3^-$ .** The influence of the initial nitrate concentration on the degradation kinetics of the model pollutant phenol and the formation of nitroaromatic and other byproducts has been investigated for three different AOPs at pH 5 and 11, respectively. Table 2 outlines the experimental layout of these experiments performed at pH 5 summarizing the most important experimental parameters and indicating whether nitrophenols were detected. Identical experiments were performed at pH 11, but no formation of nitroaromatic compounds was observed in any case. Ni-

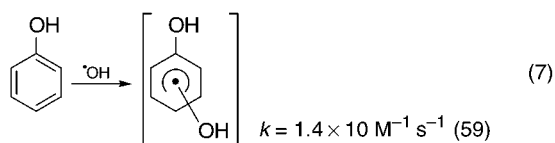
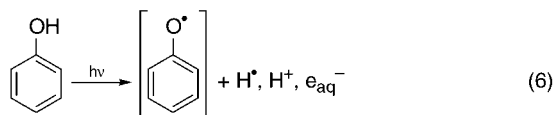
TABLE 2. Summary of Experiments at pH 5 To Study the Influence of Nitrate

process	filter	concn of NO <sub>3</sub> <sup>-</sup> (mM)	detected nitrophenols
photolysis			
photolysis		10	2-NP, 4-NP
photolysis		100	2-NP, 4-NP
H <sub>2</sub> O <sub>2</sub> /UV			
H <sub>2</sub> O <sub>2</sub> /UV		10	
H <sub>2</sub> O <sub>2</sub> /UV		100	2-NP
TiO <sub>2</sub> /UV	320		
TiO <sub>2</sub> /UV	320	10	
TiO <sub>2</sub> /UV	320	100	
TiO <sub>2</sub> /UV		10	
TiO <sub>2</sub> /UV		100	

trophenols are formed only when homogeneous processes are employed as the AOP. For the H<sub>2</sub>O<sub>2</sub>/UV process the formation of nitrophenols occurred only when the concentration of nitrate was higher than the initial concentration of H<sub>2</sub>O<sub>2</sub>. For the heterogeneous TiO<sub>2</sub>/UV process the formation of nitrophenols is completely suppressed, even when no 320-nm cutoff filter was used in the light path enabling in principle the direct excitation of nitrate and phenol. While at pH 5 only hydroquinone, benzoquinone, and hydroxybenzoquinone were detected as intermediates, considerably higher amounts and concentrations were found when homogeneous processes were employed. Highest concentrations were detected for the direct photolysis, while with H<sub>2</sub>O<sub>2</sub>/UV being the oxidation process slightly smaller concentrations of intermediates were observed in comparison to the direct photolysis. Besides the intermediates mentioned above, the formations of trihydroxybenzenes, 2,5,4'-trihydroxybiphenyl, and 2- and 4-nitrophenol were observed. Especially the latter compounds are known to have a considerably higher toxicity to organisms than phenol itself: e.g., the oral LD<sub>50</sub> values for mice are phenol, 3.5 g kg<sup>-1</sup>; 2-NP, 1.297 g kg<sup>-1</sup>; and 4-NP, 0.467 g kg<sup>-1</sup> (56, 57).

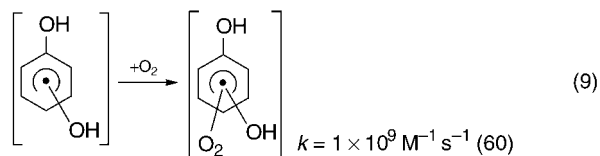
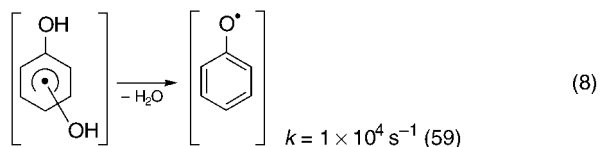
## Discussion

**Formation of Nitrophenols.** Direct excitation of phenol by light leads to the formation of solvated electrons, hydrogen atoms, and phenoxyl radicals (58) (eq 6), and its reaction with •OH radicals leads to the formation of dihydroxycyclohexadienyl radicals (eq 7).

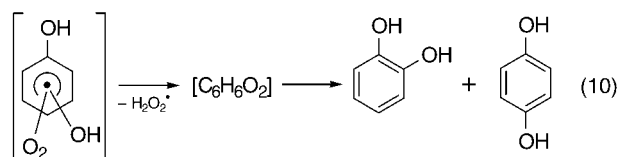


Subsequent reactions of the dihydroxycyclohexadienyl radical lead either to the formation of phenoxyl radicals by the elimination of water (eq 8) or to the formation of peroxy radicals by the addition of molecular oxygen (eq 9). The former reaction is acid/base-catalyzed. Thus, only in neutral solution the elimination of water from the •OH adduct is as slow as reported (59).

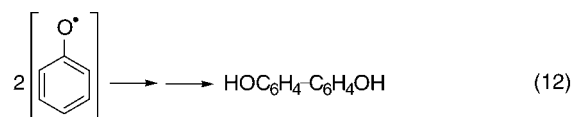
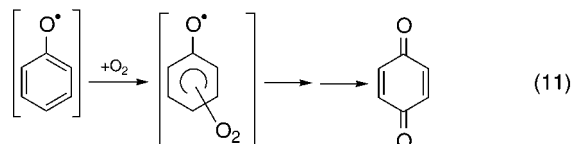
Peroxy radicals are known to eliminate in an unimolecular reaction superoxide radicals resulting after the rearrangement of the aromatic system in the formation of hydroquinone



and catechol (eq 10). Micic et al. (61) reported that the rearrangement of the aromatic system is the slowest step in this reaction sequence ( $k = 26.7 \text{ s}^{-1}$ ).



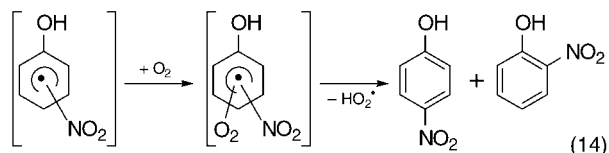
The reaction of phenoxyl radicals with molecular oxygen will most probably result in the formation of benzoquinone (eq 11). However, the reaction rate of oxyl radicals with dioxygen is very small (62), and only with electron-rich phenoxyl radicals can this rate be measured (63). An undesired side reaction is the dimerization of these radicals forming hydroxylated biphenyls (eq 12). Reaction 12 is favored by decreasing the molecular oxygen concentration, but even under saturation with O<sub>2</sub> the formation of dihydroxybiphenyls has been observed in the aqueous phase (64).



In the presence of nitrogen dioxide several side reactions can be postulated in addition to the classical photochemical degradation reactions of phenol which are suitable to explain the formation of nitrophenols. The first possibility is the addition of a NO<sub>2</sub>• radical to the aromatic ring (eq 13) followed by the addition of O<sub>2</sub> and the elimination of a superoxide radical resulting in the formation of nitrophenols (eq 14). Since reaction 7 is a diffusion-controlled reaction, the formation of nitrophenols via reactions 13 and 14 can only be explained if the rate constant for reaction 13 is of the same order of magnitude as that of the reaction of phenol with •OH radicals (eq 7).

A second possibility leading finally to the formation of nitrophenols is the reaction of a dihydroxycyclohexadienyl radical with nitrogen dioxide (eq 4b). However, in the presence of molecular oxygen, the proposed reaction of the dihydroxycyclohexadienyl radical with nitrogen dioxide will be of minor importance, since nitrogen dioxide will only attain a very low steady-state concentration. Therefore, this possibility for the formation of nitrophenols appears to be rather unlikely in comparison to the reaction sequence discussed before. Furthermore, Sarakha et al. (31) showed

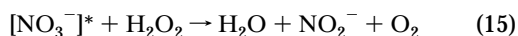




that the formation of nitroaromatic intermediates was not influenced by the presence of  $\cdot\text{OH}$  radical scavengers. Thus, reaction 4b indeed can be neglected in comparison to reaction 13.

**Influence of Reaction pH.** It was a result of this study that the formation of nitrophenols as intermediates occurred only at pH 5, while at pH 11 no nitrophenols were detected. Since the nitrite radical is most likely an electrophilic radical, it should react much faster with phenolates than with phenols. Thus, at pH values above the  $\text{p}K_a$  of phenol ( $\text{p}K_a = 9.89$ ) the electron-transfer reaction leading to the formation of nitrite and phenoxy radicals (eq 5) should become the predominant reaction for the quenching of  $\text{NO}_2^*$  radicals, while this reaction will be negligible below the  $\text{p}K_a$  of phenol. Consequently, the reaction rate for reaction 13 must be significantly smaller at pH 11 than at pH 5, and the formation of nitroaromatic intermediates is strongly influenced by the reaction pH. Additionally,  $\text{NO}_2^*$  radicals can be scavenged by solvated electrons generated from the photolysis of phenol (eq 6).

**Influence of  $\text{H}_2\text{O}_2$ .** The formation of nitroaromatic byproducts was successfully suppressed when the concentration of nitrate ions was not higher than that of hydrogen peroxide. Only when the  $\text{NO}_3^-$  concentration was significantly higher were traces of nitrophenols detected. In the presence of  $\text{H}_2\text{O}_2$  and due to its photolysis by UV light, higher concentrations of hydroxyl radicals are formed. Thus, all reactions employing  $\cdot\text{OH}$  radicals should be favored, and the oxidative destruction of phenol (eq 7) will become more important than the reaction of phenol with  $\text{NO}_2^*$  radicals (eq 13). On the other hand, higher concentrations of  $\cdot\text{OH}$  radicals should as well result in higher concentrations of nitrogen dioxide (eq 3), and consequently no net beneficial effect in favor of the oxidation of phenol via hydroxyl radicals should be expected. However, under the employed experimental conditions (phenol, 1 mM,  $\epsilon_{254} = 218.7 \text{ L mol}^{-1} \text{ cm}^{-1}$ ;  $\text{H}_2\text{O}_2$ , 10 mM,  $\epsilon_{254} = 18.7 \text{ L mol}^{-1} \text{ cm}^{-1}$ ;  $\text{NO}_3^-$ , 100 mM,  $\epsilon_{254} = 3.0 \text{ L mol}^{-1} \text{ cm}^{-1}$ ), only about 25% of the available photons will result in the direct photolysis of hydrogen peroxide, i.e., the sum of the individual absorption coefficient times the quantum yield of  $\cdot\text{OH}$  radical generation. Therefore, the additional production of  $\cdot\text{OH}$  radicals via photolysis of  $\text{H}_2\text{O}_2$  plays a minor role, and the prevailing reaction must be the scavenging of excited nitrate ions by hydrogen peroxide (eq 15). Thus, the most important function of hydrogen peroxide in this synthetic model wastewater is not the enhancement of the degradation of phenol by the additional formation of hydroxyl radicals but the suppression of the formation of nitroaromatic byproducts by preventing photolytic reactions of nitrate.



**Influence of  $\text{TiO}_2$ .** Titanium dioxide efficiently suppresses the formation of nitrophenols in detectable amounts under all experimental conditions examined in this study. Several models can be considered to explain this observation. The most obvious reason is the inner filter effect of the photocatalyst. Titanium dioxide in its anatase modification is

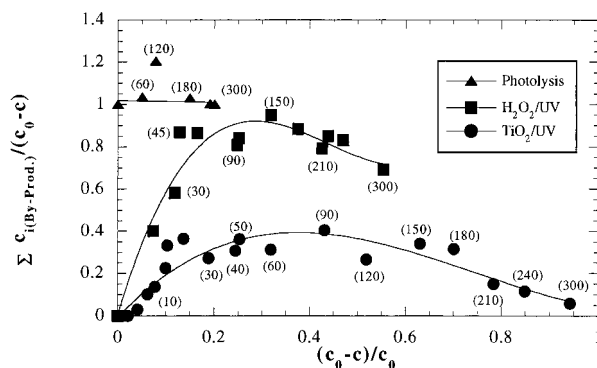


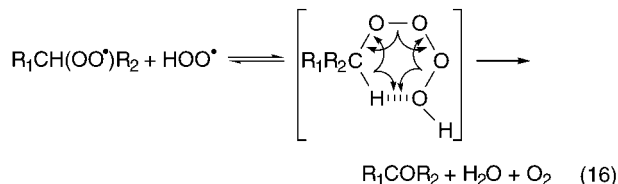
FIGURE 5. Plot of the degree of nonmineralized intermediates to the overall amount of converted phenol as a function of the degraded amount of phenol for the photochemical oxidation of phenol with different AOPs. The numbers in brackets indicate the corresponding irradiation times. Experimental conditions: 1 mM phenol, 100 mM  $\text{KNO}_3$ , continuous  $\text{O}_2$  stream,  $I \sim 320 \mu\text{W min}^{-1}$ , 293 K,  $V = 150 \text{ mL}$ , irradiation time = 300 min, 5 g  $\text{L}^{-1}$  Degussa P25 for the  $\text{TiO}_2/\text{UV}$  process and 10 mM  $\text{H}_2\text{O}_2$  for the  $\text{H}_2\text{O}_2/\text{UV}$  process.

absorbing light below 388 nm. Thus, with the employed photocatalyst concentrations (5 g  $\text{L}^{-1}$ ) any direct photolytic excitation of phenol or nitrate is almost completely suppressed. Additionally, the net amount of  $\cdot\text{OH}$  radicals will be increased in the presence of the photocatalyst, since the formation of nitrite ions by photolysis of nitrate and consequently the quenching of hydroxyl radicals via reaction 3 are suppressed and almost all generated  $\cdot\text{OH}$  radicals will be available to initiate the oxidation of phenol and its intermediates.

**Comparison of the AOPs.** For a better comparison of the three AOPs the ratio between the sum of the concentration of all detected intermediates and that of the converted phenol is plotted as a function of the amount of degraded phenol in Figure 5. The y-axis of this plot can be interpreted as the normalized degree of nonmineralized intermediates in relation to the overall amount of converted phenol. Hence, every point in this figure provides information about the degree of nonmineralized intermediates for a given value of conversion of the model pollutant phenol for all three oxidation processes; e.g., 40% of the initial phenol content has been degraded after 90 min of irradiation in the photocatalytic system, and it is also obvious from this figure that 60% of this degraded amount of phenol has already been converted to carbon dioxide, while 40% is still present in the form of nonmineralized or nondetectable intermediates. The comparison of the three AOPs provided in Figure 5 shows that within a given irradiation time of 300 min the degradation of phenol is exceeding 90% conversion with heterogeneous photocatalysis, while with  $\text{H}_2\text{O}_2/\text{UV}$  (55%) and photolysis (20%) it is considerably smaller. Furthermore, the maximum degree of nonmineralized intermediates is remarkably smaller with photocatalysis (40%) than with  $\text{H}_2\text{O}_2/\text{UV}$  (85%) or photolysis (~100%). Thus, photocatalysis employing  $\text{TiO}_2$  as the photocatalyst not only is the fastest of all three oxidation processes under comparable irradiation conditions but also produces the smallest percentage of byproducts, a point which is often neglected or even ignored when comparing different oxidation processes.

Another remarkable result which can be extracted from Figure 5 is the observation that the ratio of nonmineralized intermediates to the overall amount of converted phenol is increasing within the first 45 min of irradiation for photocatalysis and for the hydrogen peroxide/UV process. This result is in clear contrast to the commonly accepted opinion that in photocatalysis most pollutants are initially oxidized to intermediates with a higher oxidation state before they are totally mineralized to carbon dioxide and water. If this

would be the case, one should obtain a ratio of nonmineralized intermediates to the overall amount of converted phenol being close to unity at the beginning of the irradiation and slowly decreasing with progressive irradiation, since phenol is degraded faster than its intermediates and almost no mineralization occurs at the beginning of irradiation. However, a close inspection of the results shown in Figure 5 shows that this is obviously not the case. On the basis of the latter result, additional degradation pathways for the photocatalytic decomposition of organic pollutants have to be considered. The first attack of an  $\cdot\text{OH}$  radical will lead to a radical intermediate which obviously readily decays via several radical and/or very reactive species directly to carbon dioxide or undetectable intermediates, respectively. Thus, the formation of stable intermediates, e.g., hydroquinone and benzoquinone during the photocatalytic degradation of phenol, can most likely be attributed to side reactions such as the quenching of radical intermediates by radical scavengers. In support of this model Mills et al. have recently reported that for the photocatalytic oxidation of 4-chlorophenol the direct oxidation to carbon dioxide via unstable intermediates amounts to 42% of the overall reaction (65). Heller and co-workers have proposed a degradation mechanism for the heterogeneous photocatalysis involving the formation of a very reactive tetraoxide. The decay of the latter would in the case of aromatic pollutants directly lead to the formation of ring-opening products such as aldehydes and alcohols (66–68). This reaction sequence is well-known in homogeneous radiation chemistry as the Russell mechanism (eq 16) (60, 68). The results by Stafford et al. (55), Mills et al. (65), and Hoffmann et al. (20) together with the results presented in this study clearly indicate that reactions such as the Russell mechanism also seem to play an important role in the heterogeneous degradation of pollutants by titanium dioxide.



## Acknowledgments

Financial support by the European Communities (Contract CII-CT94-0035) is gratefully acknowledged.

## Literature Cited

- Alloway, B.; Ayres, D. *Chemical Principles of Environmental Pollution*, 1st ed.; Blackie Academic & Professional: London, 1993; p 1.
- Ballschmitter, K. *Pure Appl. Chem.* **1996**, *68*, 1771.
- Simonich, S.; Hites, R. *Science* **1995**, *269*, 1851.
- Seel, P.; Knepper, T.; Gabriel, S.; Weber, A.; Haberer, K. *Vom Wasser* **1994**, *83*, 357.
- Häfner, M. *Nature* **1989**, *10*, 20.
- Legrini, O.; Oliveros, E.; Braun, A. *Chem. Rev.* **1993**, *93*, 671 and further references therein.
- Bahnmann, D.; Cunningham, J.; Fox, M. A.; Pelizzetti, E.; Serpone, N. In *Aquatic and Surface Photochemistry*; Helz, G. R., Zepp, R. G., Crosby, D. G., Eds.; Lewis Publishers: Boca Raton, FL, 1994; pp 261–317 and further references therein.
- Pelizzetti, E.; Minero, C.; Pramauro, E. In *Chemical Reactor Technology for Environmentally Safe Reactors and Products*; de Lasa, H., Ed.; Kluwer Academic Publishers: Netherlands, 1993; pp 577–608 and further references therein.
- Blake, D. M. *Bibliography of Work on the Photocatalytic Removal of Hazardous Compounds from Water and Air*; National Renewable Energy Laboratory, 1994.
- Annee, J.; Logemann, F. In *Oxidation Technologies for Water and Wastewater Treatment*; Vogelpohl, A., Ed.; CUTEC-Schriftenreihe No. 23; 1996.
- Jochimsen, J.; Jekel, M. In *Oxidation Technologies for Water and Wastewater Treatment*; Vogelpohl, A., Ed.; CUTEC-Schriftenreihe No. 23; 1996.
- Kayser, R. In *Oxidation Technologies for Water and Wastewater Treatment*; Vogelpohl, A., Ed.; CUTEC-Schriftenreihe No. 23; 1996.
- Bekkölet, M.; Lindner, M.; Weichgrebe, D.; Bahnmann, D. *Solar Energy* **1996**, *56*, 455.
- Heller, A.; Nair, M.; Davidson, L.; Luo, Z.; Schwitzgebel, J.; Norrell, J.; Brock, J.; Lindquist, S.; Ekerdt, J. In *Photocatalytic Purification and Treatment of Water and Air*; Ollis, D., Al-Ekabi, H., Eds.; Elsevier Science Publishers BV: The Netherlands, 1993; pp 139–153.
- Weichgrebe, D.; Vogelpohl, A.; Bockelmann, D.; Bahnmann, D. In *Photocatalytic Purification and Treatment of Water and Air*; Ollis, D., Al-Ekabi, H., Eds.; Elsevier Science Publishers BV: The Netherlands, 1993; pp 579–584.
- Sabin, F.; Türk, T.; Vogler, A. *Z. Wasser-Abwasser-Forsch.* **1992**, *25*, 163.
- Bockelmann, D.; Lindner, M.; Bahnmann, D. In *Fine Particles Science and Technology*; Pelizzetti, E. Ed.; Kluwer Academic Publishers: The Netherlands, 1996; pp 675–689.
- Abdullah, M.; Low, G.; Matthews, R. W. *J. Phys. Chem.* **1990**, *94*, 6820.
- Simmons, M. S.; Zepp, R. G. *Water Res.* **1986**, *20*, 899.
- Hoffmann, M.; Martin, S.; Choi, W.; Bahnmann, D. *Chem. Rev.* **1995**, *95*, 69 and further references therein.
- Sclafani, A.; Palmisano, L. *Gazz. Chim. Ital.* **1990**, *120*, 599.
- Wagner, I.; Strehlow, H.; Busse, G. *Z. Phys. Chem. (Wiesbaden)* **1980**, *123*, 1 and further references therein.
- Kotzias, D.; Parlar, H.; Korte, F. *Naturwissenschaften* **1982**, *69*, 444.
- Zepp, R.; Hoigne, J.; Bader, H. *Environ. Sci. Technol.* **1987**, *21*, 443.
- Mark, G.; Korth, H.; Schuchmann, H.; von Sonntag, C. *J. Photochem. Photobiol. A: Chem.* **1996**, *101*, 89.
- Meyerstein, D.; Treinin, A. *Trans. Faraday Soc.* **1961**, *57*, 2104.
- Bayliss, N.; Bucat, R. *Aust. J. Chem.* **1975**, *28*, 1865.
- Warneck, P.; Wurzinger, C. *J. Phys. Chem.* **1988**, *92*, 6278.
- Zellner, R.; Exner, M.; Herrmann, H. *J. Atmos. Chem.* **1987**, *10*, 411.
- Buxton, G.; Greenstock, C.; Helman, W.; Ross, A. *J. Phys. Chem. Ref. Data* **1988**, *17*, 513.
- Sarakha, M.; Boule, P.; Lenoir, D. *J. Photochem. Photobiol. A: Chem.* **1993**, *75*, 61.
- Suzuki, J.; Okazaki, H.; Sato, T.; Suzuki, S. *Chemosphere* **1982**, *11*, 437.
- Bunce, N.; Cater, S.; Willson, J. *J. Chem. Soc., Perkin Trans. 2* **1985**, 2013.
- Suzuki, J.; Sato, T.; Ito, A.; Suzuki, S. *Bull. Environ. Contam. Toxicol.* **1990**, *45*, 516.
- Russi, H.; Kotzias, D.; Korte, F. *Chemosphere* **1982**, *11*, 1041.
- Niessen, R.; Lenoir, D.; Boule, P. *Chemosphere* **1988**, *10*, 1977.
- Bandow, H.; Washida, N.; Akimoto, H. *Bull. Chem. Soc. Jpn.* **1985**, *58*, 2531.
- Knispel, R.; Koch, R.; Siese, M.; Zetzsch, C. *Ber. Bunsen-Ges. Phys. Chem.* **1990**, *94*, 1375.
- Moschonas, N.; Danalatos, D.; Glavas, S. *Monatsh. Chem.* **1996**, *127*, 875.
- Alfassi, Z.; Huie, R.; Neta, P.; Shoute, L. *J. Phys. Chem.* **1990**, *94*, 8800.
- Degussa Tech. Bull. **1984**, *56*, 8.
- Bickley, R.; Gonzalez-Carreno, T.; Lees, J.; Palmisano, L.; Tilley, R. *J. Sol. State Chem.* **1991**, *92*, 178.
- Bahnmann, D.; Bockelmann, D.; Goslich, R. *Solar Energy Mater.* **1991**, *24*, 564.
- Heller, H. G.; Langan, J. R. *J. Chem. Soc., Perkin Trans. 2* **1981**, 341.
- Serpone, N.; Terzian, R.; Lawless, D.; Kennepohl, P.; Sauvé, G. *J. Photochem. Photobiol. A: Chem.* **1993**, *73*, 11.
- Tahiri, H.; Serpone, N.; Le van Mao, R. *J. Photochem. Photobiol. A: Chem.* **1996**, *93*, 199.
- Serpone, N.; Sauvé, G.; Koch, R.; Tahiri, H.; Pichat, P.; Piccinini, P.; Pelizzetti, E.; Hidaka, H. *J. Photochem. Photobiol. A: Chem.* **1996**, *94*, 191.
- Schuchmann, M. N.; Bothe, E.; von Sonntag, J.; von Sonntag, C. *J. Chem. Soc., Perkin Trans. 2* **1998**, 791.
- Okamoto, K.; Yamamoto, Y.; Tanaka, H.; Tanaka, M.; Itaya, A. *Bull. Chem. Soc. Jpn.* **1985**, *58*, 2015.
- Augugliaro, V.; Palmisano, L.; Sclafani, A.; Minero, C.; Pelizzetti, E. *Toxicol. Environ. Chem.* **1988**, *16*, 89.
- Kawaguchi, H. *Environ. Technol. Lett.* **1984**, *5*, 471.

- (52) Matthews, R. W.; McEvoy, S. R. *J. Photochem. Photobiol. A: Chem.* **1992**, *64*, 231.
- (53) Trillas, M.; Pujol, M.; Domenech, X. *J. Chem. Technol. Biotechnol.* **1992**, *55*, 85.
- (54) Theurich, J.; Lindner, M.; Bahnemann, D. *Langmuir* **1996**, *12*, 6368.
- (55) Stafford, U.; Gray, K. A.; Kamat, P. V. *J. Phys. Chem.* **1994**, *98*, 6343.
- (56) Allan, R. E. In *Patty's Industrial Hygiene and Toxicology*, 4th ed.; Clayton, G. D., Clayton F. E., Eds.; John Wiley & Sons Inc.: New York, 1994; Vol. 2, Part B, Chapter 24.
- (57) Benya, T. J.; Cornish, H. H. In *Patty's Industrial Hygiene and Toxicology*, 4th ed.; Clayton, G. D., Clayton F. E., Eds.; John Wiley & Sons Inc.: New York, 1994; Vol. 2, Part B, Chapter 16.
- (58) Jin, F.; Leitich, J.; von Sonntag, C. *J. Photochem. Photobiol. A: Chem.* **1995**, *92*, 147.
- (59) Land, E.; Ebert, M. *Trans. Faraday Soc.* **1967**, *63*, 1181.
- (60) von Sonntag, C.; Schuchmann, H. *Angew. Chem., Int. Ed. Engl.* **1991**, *30*, 1229–1253.
- (61) Micic, O.; Nenadovic, M. *J. Phys. Chem.* **1976**, *80*, 940.
- (62) Jin, F.; Leitich, J.; von Sonntag, C. *J. Chem. Soc., Perkins Trans. 2* **1993**, 1583.
- (63) Wang, D.; Gyoergy, I.; Hildenbrand, K.; von Sonntag, C. *J. Chem. Soc. Perkin Trans. 2* **1994**, 45.
- (64) Sato, K.; Takimoto, K.; Tsuda, S. *Environ. Sci. Technol.* **1978**, *12*, 1043.
- (65) Mills, A.; Morris, S.; Davies, R. *J. Photochem. Photobiol. A: Chem.* **1993**, *70*, 183.
- (66) Heller, A. *Acc. Chem. Res.* **1995**, *28*, 503.
- (67) Schwitzgebel, J.; Ekerdt, J.; Gerischer, H.; Heller, A. *J. Phys. Chem.* **1995**, *99*, 5633.
- (68) Sitkiewitz, S.; Heller, A. *New J. Chem.* **1996**, *20*, 233.
- (69) Russell, G. *J. Am. Chem. Soc.* **1957**, *79*, 3871.

*Received for review April 9, 1998. Revised manuscript received September 29, 1998. Accepted October 15, 1998.*

ES980358J